ADVANCED MATERIALS

Supporting Information

for *Adv. Mater.*, DOI: 10.1002/adma.201902189

High-Throughput Growth of Microscale Gold Bicrystals for Single-Grain-Boundary Studies

*Lucia T. Gan, Rui Yang, Rachel Traylor, Wei Cai, William D. Nix, and Jonathan A. Fan**

Supporting Information

High-Throughput Growth of Microscale Gold Bicrystals for Single-Grain-Boundary Studies

*Lucia T. Gan, Rui Yang, Rachel Traylor, Wei Cai, William D. Nix, and Jonathan A. Fan**

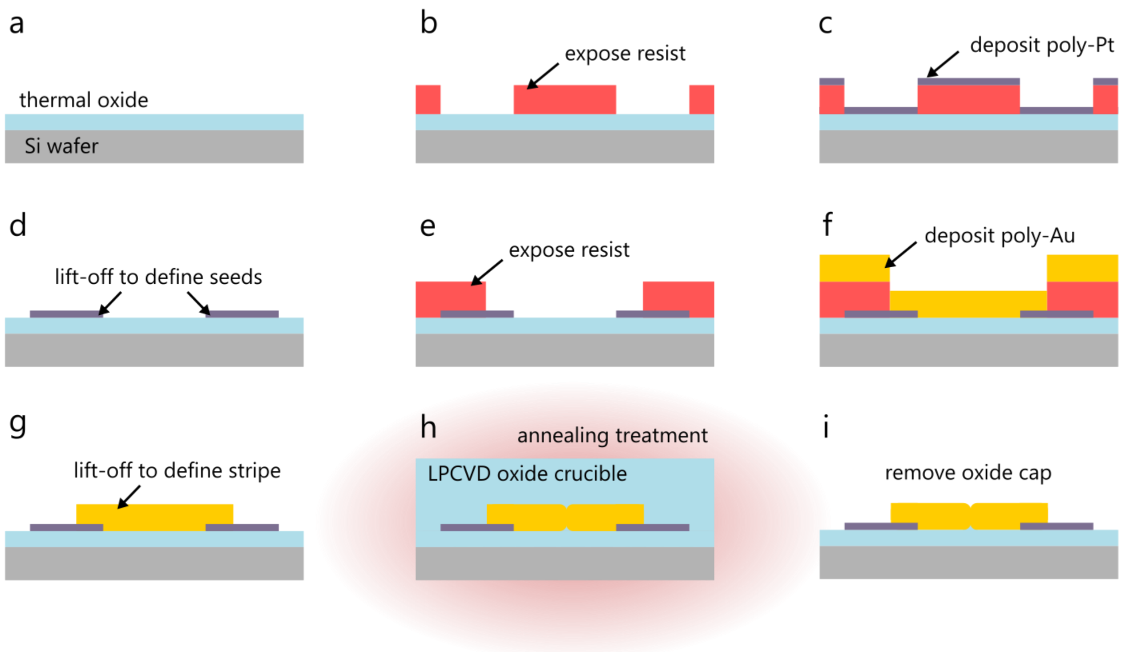

Figure S1. Schematic illustrations of the fabrication procedure for preparing bicrystal structures. a) Growth of 300-nm-thick thermal oxide layers on a (100) single crystal p-type silicon wafer. b) Photolithography followed by c) electron beam evaporation of a 30-nm-thick platinum metal film is performed to pattern the seeds. d) Metal lift-off defines platinum seeds that are 10 µm by 10 µm. e) Second photolithography step followed by f) electron beam evaporation of 100-nm-thick gold metal film patterns the stripes. g) Metal lift-off defines gold stripes 4 µm wide and 40 to 160 µm long. h) Low-pressure chemical vapor deposition (LPCVD) of 3-µm-thick silicon dioxide layers to form a crucible, followed by rapid thermal annealing on the structures, using the annealing schedule described in Figure 1b. i) Removal of the oxide cap through dry etching reveals the bicrystal structures.

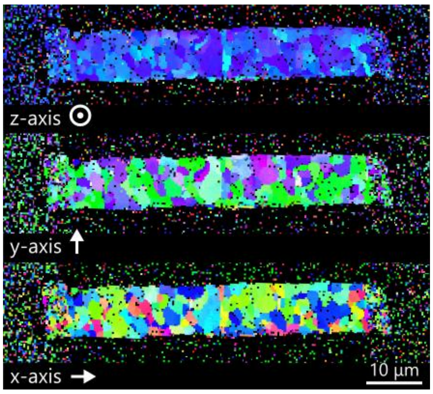

Figure S2. EBSD maps in the z-, y-, and x-sample-axes of the metal microstructure heated to a peak temperature of 900˚C using the same 15°C per second heating and cooling parameters described in Figure 1b. While grain growth does occur, the gold remains polycrystalline after this annealing treatment. Bicrystal formation occurs only when the peak temperature exceeds gold's melting temperature such that the gold transitions to its liquid phase.

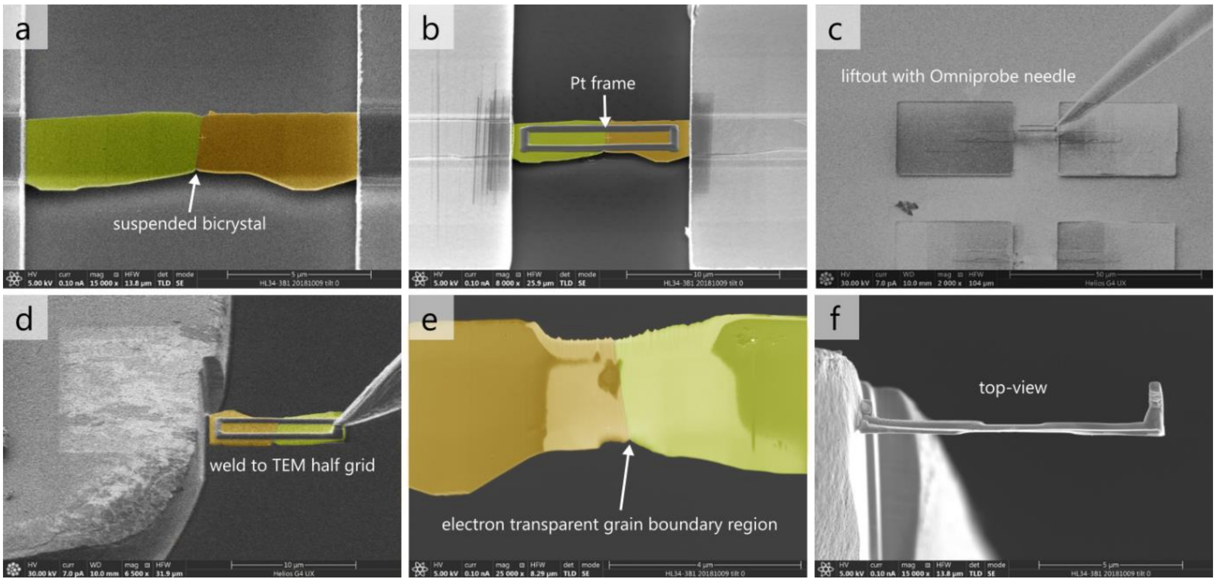

Figure S3. False-colored SEM images showing the preparation steps of the top-view TEM samples enabled by the unique metal-on-insulator crystal growth process. a) Suspended bicrystals fabricated by undercutting the underlying oxide substrate through HF vapor etching. b) Thin-film suspended structure stabilized with a platinum-deposited frame. c) Bicrystal lifted out by a nanomanipulator after focused ion beam milling. d) Bicrystal mounted to a TEM half grid. e) The region around the grain boundary is thinned using a focused ion beam until it is electron transparent. f) Top-view SEM image showing that the transparent grain boundary region is straight, thinned, and ready for subsequent TEM analysis.

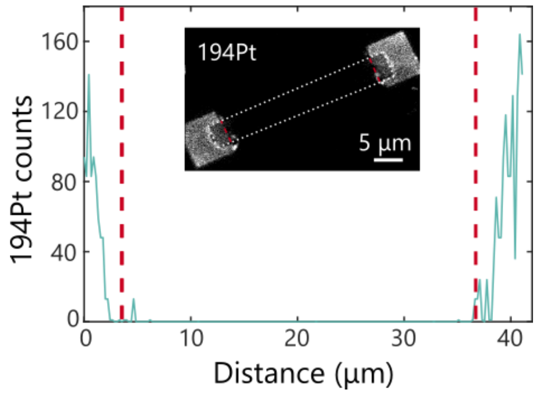

Figure S4. NanoSIMS compositional analysis shows that there is no discernable platinum in the stripe outside of the seed region when the gold microstructure is heated to a peak temperature of 900˚C. The structures are annealed using the same 15°C per second heating and cooling parameters described in Figure 1b. Long-range platinum diffusion occurs only when the gold is in the liquid phase.

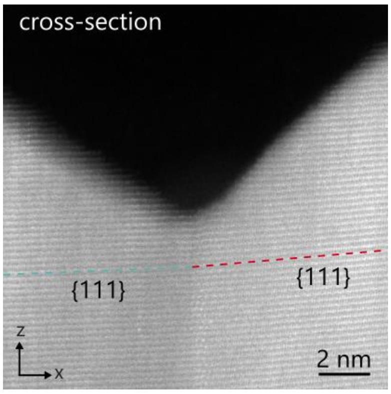

Figure S5. Bicrystals form surface grooves normal to the substrate, seen in the HRSTEM cross-section image. The horizontal lattice fringes correspond to (111) planes parallel to the metal-oxide interface.

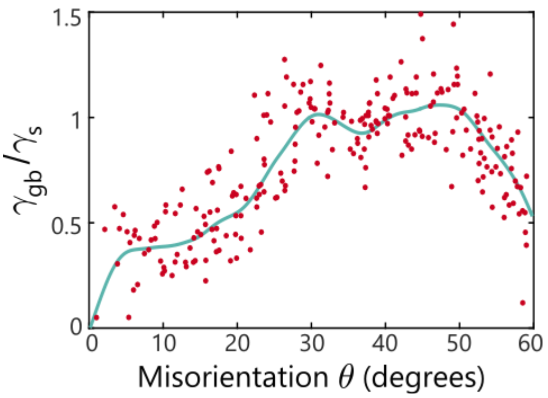

Figure S6. Plot of the mean relative grain boundary energy γ_{gb}/γ_s as a function of misorientation angle θ, as shown by the solid line. The full dataset is given by the discrete red data points.